Carbohydrate Polymers 85 (2011) 201–207

Contents lists available at ScienceDirect

Carbohydrate Polymers

journal homepage: www.elsevier.com/locate/carbpol

Physical characterization of arabinoxylan powder and its hydrogel containing a methyl xanthine

Sherry Iravani[a], Colin S. Fitchett[b], Dominique M.R. Georget[a,*]

[a] School of Chemistry, University of East Anglia, Norwich, Norfolk, NR4 7TJ, UK
[b] Cambridge Biopolymers Ltd., Ickleton Road, Duxford, Cambridgeshire, CB22 4FB, UK

ARTICLE INFO

Article history:
Received 9 August 2010
Received in revised form 7 February 2011
Accepted 9 February 2011
Available online 15 February 2011

Keywords:
Maize bran
Arabinoxylans
Hydrogel
Caffeine
Drug release

ABSTRACT

Arabinoxylan powder has been characterized using TGA, FT-IR, MTDSC, SEM and particle size analysis. Results showed that particle size distribution was bimodal with peaks at 61 μm and 599 μm. Particles were irregular in shape and surface. Thermal analysis revealed an endothermic event at 70.9 °C due to water loss followed by the glass transition temperature at 198.8 °C. The decomposition temperature was detected at 303 °C. Arabinoxylan hydrogels including caffeine were prepared by peroxidase/peroxide oxidative cross-linking. The mechanical properties determined at various content of peroxidase showed the force at failure, the deformation at failure and the cohesiveness to decrease slightly for peroxidase concentration greater than 264 μg/g (polysaccharide basis). The hydrogels swelling was greater in distilled water than in 0.1 M HCl after 3 h. The caffeine release was the greatest in acidic pH. The dissolution profiles were modelled using the Higuchi, Ritger and Peppas and Peppas and Sahlin equations to explain the mechanism of drug release.

1. Introduction

Arabinoxylan (AX) is a family of branched, non-starch polysaccharides present in the cell wall of maize bran (Saulnier & Thibault, 1999). They are also present as water extractable and water unextractable polymers in the endosperm of cereal grains such as wheat (Courtin & Delcour, 2001; Saulnier, Sado, Branlard, Charmet, & Guillon, 2007). These polysaccharides contain mainly arabinose and xylose residues, the α-L-arabinofuranosyl units are attached at O-2 and/or O-3 position along the (1 → 4)-β-D-xylan backbone. Ferulic acid in the order of 0.7% of the cell wall (Ng, Greenshields, & Waldron, 1997) is esterified to arabinose units and produces dimers that cross-link arabinoxylan chains together (Grabber, Ralph, & Hatfield, 2000). Dimerisation occurs via a radical, oxidative mechanism, using enzymatic free radical oxidative agents (laccase or peroxidase-H_2O_2) to form mainly 8-5-, 8-O-4-, 5-5-, 8-8-, and 4-O-5-coupled dehydrodiferulates (Bunzel, Ralph, Funk, & Steinhart, 2005; Carvajal-Millan, Landillon et al., 2005). The ratio of Ara:Xyl determines the properties of arabinoxylan hydrogel (Carvajal-Millan, Guilbert, Doublier, & Micard, 2006) and is 0.85 (Niño-Medina et al., 2010) for arabinoxylan extracted from maize bran.

The applications of this family of polysaccharides are gradually expanding. Indeed films fabricated from these biopolymers as potential packaging have been prepared and tested (Höije, Sternemalm, Heikkinen, Tenkanen, & Gatenholm, 2008; Péroval, Debeaufort, Despré, & Voilley, 2002). Fibres for wound dressing were also considered and optimized and showed some promise (Miraftab, Qiao, Kennedy, Anand, & Groocock, 2003).

Interestingly studies on the use of AX hydrogels for the release of active molecules for biomedical applications are progressively emerging. In the last few years, the work from Carvajal-Millan, Guilbert et al. (2005), Carvajal-Millan, Landillon et al., 2005 and Berlanga-Reyes et al. (2009) demonstrated that AX hydrogels formed via the oxidative cross-linking using laccase could be employed for controlled release of model proteins. This system presents several benefits. Polysaccharide based hydrogels are natural, non-toxic and highly biocompatible. Hence they would be good candidates for the design of novel drug delivery systems. In the case of AX polysaccharides, their hydrogels contain ferulic acid which demonstrates antioxidant and anticancer properties (Ebringerová & Heinze, 2000). Further they possess cholesterol lowering activities (Ou & Kwok, 2004). Entrapment of molecules of therapeutic activity within polysaccharide based hydrogels by enzymatic cross-linking is very novel. However the capacity for AX hydrogel to incorporate and release active ingredients has not been explored fully. From a manufacture perspective, the formation of AX hydrogel is straightforward when compared to more complex chemically modified polymers already available. Consequently

* Corresponding author. Tel.: +44 01603 592029; fax: +44 01603 592003.
E-mail address: d.georget@uea.ac.uk (D.M.R. Georget).

0144-8617/$ – see front matter © 2011 Elsevier Ltd. All rights reserved.
doi:10.1016/j.carbpol.2011.02.017

these hydrogels would pave the way to design safe, biocompatible and sustainable encapsulation systems for biomedical applications (Vázquez et al., 1992).

Previous studies have characterized the physical and dissolution properties of AX hydrogels containing proteins but scarce information is available on the inclusion of low molecular weight, simpler active ingredient and its release from AX hydrogels. Little is also known on the physical properties of AX powder which are important attributes from a manufacture point of view. If this material is to be exploited and to find its niche on the market, it is of paramount importance to investigate the physical properties of its powder form. In the current study, the possibility of using AX hydrogel for oral delivery of a methyl xanthine i.e., caffeine was investigated. Firstly the physical properties of AX powder were determined. Secondly AX hydrogels were produced with the inclusion of caffeine as a model molecule via oxidative cross-linking using peroxidase/H_2O_2. Their high deformation mechanical properties were assessed. The hydrogel swelling and the caffeine release in acidic medium and distilled water were tested and modelled with a view to predict the behaviour of the AX hydrogels in the gastrointestinal tract.

2. Materials and methods

2.1. Materials and hydrogel preparation

AX from maize bran corresponding to the water extractable fraction was supplied by Cambridge Biopolymers Limited, Cambridge with a molecular weight ranging between 90 and 500 kDa and with the following composition: xylose, 42%, arabinose, 34%, galactose, 11%, glucose, 11%, glucuronic acid, 1.2% and ferulic acid 0.4%. In this study AX powder will be referred to the raw material from the supplier. Horseradish type I peroxidase enzyme (113 purpurogallin units/mg), hydrogen peroxide (35% (w/v)) and caffeine (98.5% pure) were purchased from Sigma–Aldrich Company Ltd., Gillingham, UK.

The preparation of AX hydrogels was a modification of the method used by Ng et al. (1997). The AX hydrogels were prepared using 50 ml AX solution (2.0% (w/v)) left to mix for 2 h after which 220 μl of horseradish peroxidase solution (400 μg/ml) corresponding to 10 units activity (88 μg of peroxidase per gram of AX) and 100 μl hydrogen peroxide (3% (w/w)) were added.

To produce caffeine loaded AX hydrogels, 54 mg caffeine (98.5% pure) was added to 50 ml of AX solution (2.0% (w/v) AX) and left for 30 min on a magnetic stirrer. Peroxidase and hydrogen peroxide were added to the AX/caffeine solution as previously described. Gels were allowed to form for 2 h at 25 °C and left in a fridge to be tested the following day.

Hydrogels were also lyophilised for 2 days using a VirTis AdVantage 2.0 benchtop freeze-dryer (SPS Scientific, Ipswich, Suffolk, UK).

2.2. Thermogravimetric analyzer (TGA)

The change in the weight of AX powder when heated was determined using a thermogravimetic analyzer TA Instruments HI-Res TGA 2950 (TA Instruments Ltd., Crawley, UK) at a heating rate of 10 °C min^{-1} to 250 °C. This allowed the water loss to be calculated when detected. The lyophilized AX hydrogel was also tested for comparison. Experiments were carried out in triplicates. Any measurements presented are the means with the standard error of the mean (sem).

2.3. Scanning electron microscopy (SEM)

AX powder sample and lyophilized AX hydrogel were mounted on aluminium pin stubs using conductive self-adhesive carbon label. The specimens were sputter coated with a layer of gold approximately 50 nm thick in a sputter coater S150B (Edwards, UK). All samples were examined in a JEOL 5900LV scanning electron microscope (JEOL Ltd., UK) at an accelerating voltage of 20 kV.

2.4. Particle size analysis

Particle size analysis was performed using a laser diffraction HELOS/BF particle size analyser (Sympatec Ltd., Bury, UK). AX powder were dispersed in sunflower oil with a stirrer speed of 1000 rpm and ultrasonicated for 5 s. Four measurements were taken at 10 s intervals to ensure reproducibility of results. The mean values and sem are presented.

2.5. Fourier transform infra-red (FT-IR) spectroscopy

Spectra were recorded on a Bruker FTIR spectrometer (Bruker Optics Limited, Coventry, UK, model IFS 66/S). AX powder and lyophilized AX hydrogels were tested. Three replicates were performed. The objective was to investigate any structural changes occurring during processing. Samples were placed on a single-reflection diamond ATR (attenuated total reflectance) accessory (SPECAC, Orpington, UK) and carefully pressed down to ensure a good contact with the ATR crystal. For each sample, 200 spectra at 2 cm^{-1} resolution were averaged. The empty ATR crystal served as a reference. Scans were performed on AX hydrogels but revealed that the spectrum was very much governed by the water. This hindered the analysis of the polysaccharide region located around the 1000 cm^{-1}. Analysis of the spectra was performed using Omnic v6.1A software (Thermo Nicolet Cooperation, Madison, USA).

2.6. Modulated temperature differential scanning calorimetry (MTDSC)

MTDSC was carried out using a TA Instruments DSC Q1000 (TA Instruments Ltd., Crawley, UK) with an attached integrated refrigerated cooling system (RCS). This instrument was operated in modulation mode. The purge gas, oxygen-free nitrogen was used to create a uniformed and stable environment within the DSC cell. The flow rate through the DSC cell was 50 mL min^{-1} and 140 mL min^{-1} through the RCS unit.

Samples were accurately weighed directly into Perkin-Elmer aluminium sample pans (No. 0219-0062) using a Mettler Toledo XS205 Dual Range balance. The sample mass used was between 3 and 4 mg. The pans were hermetically sealed using a proprietary sealing press. The samples were equilibrated at 20 °C before being heated to 250 °C with an underlying heating rate of 2 °C min^{-1} and a modulation amplitude ±0.212 °C every 40 s. The samples were then cooled down prior to undergoing a second heating cycle using the previous scanning conditions. MTDSC scans were analyzed using the software Universal Analysis (TA Instruments Ltd., Crawley, UK). MTDSC experiments were repeated three times to ensure reproducibility.

2.7. Swelling test

To investigate the effects of the dissolution medium on swelling behaviour of the AX hydrogel, the swelling test was conducted.

The AX hydrogel was prepared and kept in the fridge for 24 h. It was weighed initially (W_i) prior to immersing in 50 ml distilled water or 50 ml 0.1 M HCl for 3 h at room temperature. The swollen weight (W_s) was obtained by blotting the excess of liquid using white absorbing paper. Swelling (%) was calculated using the fol-

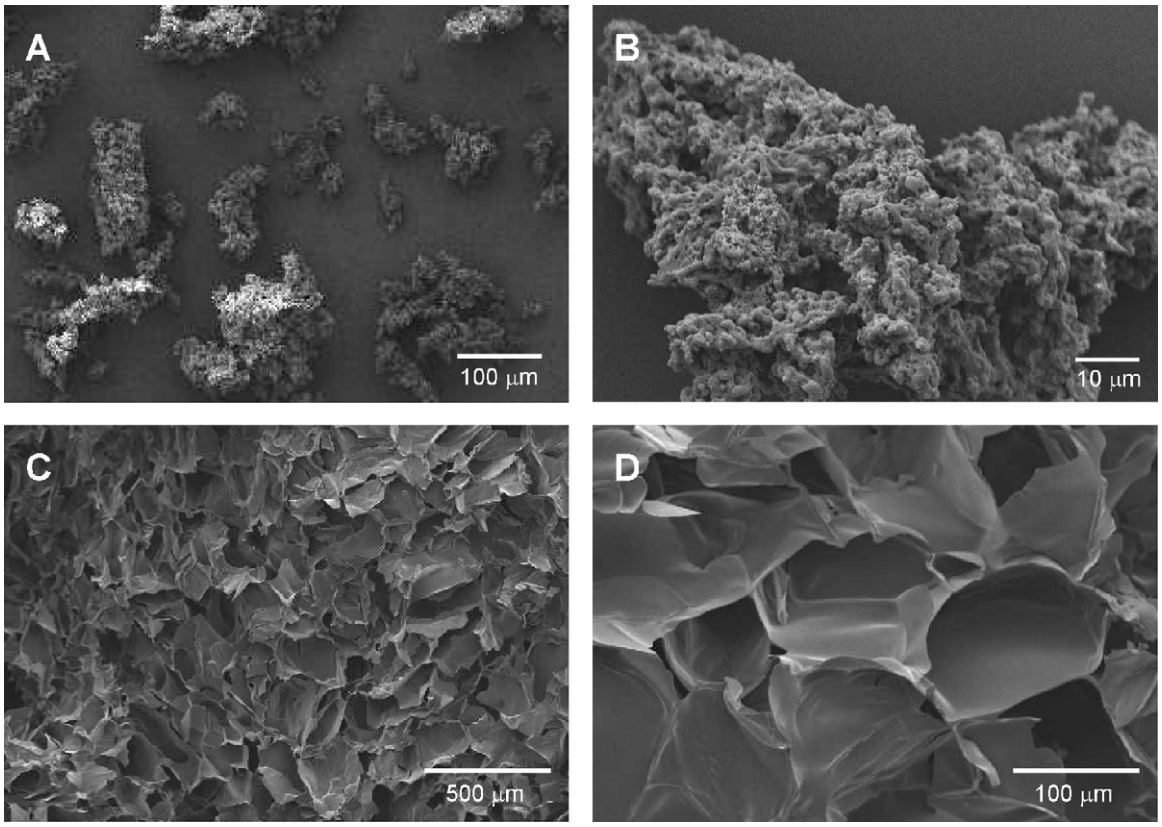

Fig. 1. SEM showing AX particles from powder (A and B) and closed honey comb like structure for lyophilised AX hydrogel containing caffeine (C and D).

lowing formula (Cao, Fu, & He, 2007)

$$\text{Swelling}\,(\%) = \frac{W_s - W_i}{W_i} \times 100$$

Mean values of three replicates and sem are presented.

2.8. Mechanical properties

The mechanical properties of the AX hydrogels cast in glass vials were measured using a Universal testing machine (Texture Analyser XTPlus, Stable Microsystems, Godalming, UK) with a 5 kg load cell in a compression mode. A metal probe with a diameter of 2.99 mm was placed above the sample surface (sample size: 25 mm height and 15 mm diameter) and then traveled at a speed of 1 mm s^{-1} until puncture of the AX hydrogel was achieved detected by a sudden drop in the force. A force/distance curve was logged using the system software (Exponent). Ten replicates were tested and values of the mean and the standard error of the mean were calculated. The force at failure, the distance at failure and the area under the curve to failure which is a measure of the cohesiveness (Sandolo, Matricardi, Alhaique, & Coviello, 2007) were extracted from the force/displacement graphs.

2.9. Dissolution properties

The release profiles of caffeine from AX hydrogels were determined using the British Pharmacopoeia (2010). Dissolution Testing Apparatus II (Copley Scientific Ltd., Nottingham, UK) was used. Hydrogel samples were prepared by transferring the cross-linked AX solution containing caffeine in 2 g suppository mould (dimension 28 mm long and maximum 13 mm diameter). This method proved to produce homogenous test specimens. One hydrogel sample placed in a mesh stainless steel basket was left to rotate in the dissolution medium. The test was performed using 900 ml of 0.1 M HCl or distilled water, at 37 ± 0.5 °C and 50 rpm. A sample (10 ml) of the dissolution medium was withdrawn from the dissolution apparatus at appropriate time intervals, and then replaced with fresh dissolution medium. The samples were filtered through a 0.22 μm syringe driven filter unit (Millipore, Cork, Ireland). Absorbance of these solutions was measured at 270 nm using S-22 Boeco UV/vis spectrophotometer (Boecol and Co., Humburg, Germany) which corresponds to λ_{max} of caffeine. Three replicates were carried out. The mean values and the sem are presented.

2.10. Curve fitting and statistical analysis

Wherever possible the data were analyzed statistically using ANOVA with the software package SPSS (SPSS UK Ltd., Woking, UK). Using a Bonferroni test, significant difference was considered at the level of $p < 0.05$. Fitting of the dissolution profiles was performed using also SPSS.

3. Results and discussion

3.1. Particle size analysis

The size distribution of AX powder, tested as is, showed a bimodal distribution with two maxima at 61.01 ± 3.73 μm and 599.28 ± 36.53 μm, respectively. The maximum at high particle size might be due to particle aggregation. The maximum at 599.28 μm was the greatest suggesting that aggregation is significant. It is also interesting to note that the dispersion was carried out in sunflower oil. Hence interactions between AX powder particles possibly hydrophilic will be favored. Therefore this would also explain the likelihood for particles to aggregate possibly via hydrogen bonds.

3.2. SEM

SEM micrographs of AX powder particles are shown in Fig. 1. The particles are irregular in shape (Fig. 1A). The approximate size that is below 100 μm is consistent with the result obtained by laser diffraction analysis. At high magnification (Fig. 1B) the particle surface appears uneven. This surface morphology could well depend on the process method or preparation as was reported by Vendruscolo et al. (2009) who prepared galactomannan using spray-drying and vacuum oven. Their SEM revealed that the surface of the vacuum oven dried material was the most irregular. This might imply that a similar phenomenon is occurring in AX particles as we know that AX powder was produced by oven drying. The SEM micrographs of the lyophilized AX hydrogels containing caffeine (Fig. 1C and D) represent the fracture surface of the material. The structure resembles that of an imperfect honey comb. The average inner diameter of the cell is approximately 100 μm. This compares well with the SEM micrographs of furcellaran reported by Tuvikene et al. (2008) who observed a closed cell foam structure for lyophilized galactan and also suggested that the cell structure would also depend on the structure and composition of the polysaccharides.

3.3. Thermal analysis

The thermal properties of AX powder and lyophilized AX hydrogels were assessed using TGA and MTDSC. Fig. 2 represents the change in weight and the first derivative for AX powder and lyophilized AX hydrogel containing caffeine as a function of temperature. Between room temperature and 100 °C, there is a decrease in weight corresponding to 6.7 ± 0.28% (wet weight basis, w.w.b) loss for the AX powder and 6.2 ± 0.27% (w.w.b) loss for lyophilized AX hydrogel. This change in weight is often in the literature associated to water evaporation or desorption below 100 °C. This also is accompanied by a peak observed at 41.1 ± 3.62 °C and 34.0 ± 0.43 °C (peak 1) detected on the first derivative profile of AX powder and lyophilized AX hydrogel, respectively. Given the difference in initial chemical composition of the two materials, it is interesting that this possible water loss is comparable. The works from Simi and Abraham (2010) and Cozic, Picton, Garda, Marlhoux, and Le Cerf (2009) on xyloglucan and Arabic gum, respectively associated this thermal event to the loss of bound water and this might be the case in arabinoxylan samples. Further above 200 °C, both samples undergo decomposition with two peaks at 286.2 ± 2.33 °C (peak 2) and 303.3 ± 2.05 °C (peak 3) for AX powder and one peak at 303.9 ± 0.78 °C for lyophilized AX hydrogel observed on the first derivative. Decomposition of xylans has been reported to undergo a two-step degradation with the first step being associated to the scission of the glycosidic bond together with degradation of the side-chain saccharides and the second step being assigned to breakage of the depolymerised fragments (Shen, Gu, & Bridgwater, 2010). In the case of lyophilized AX hydrogel, only one peak is discerned possibly indicating the hindering effect of cross-linking on the thermal decomposition of the biopolymeric network.

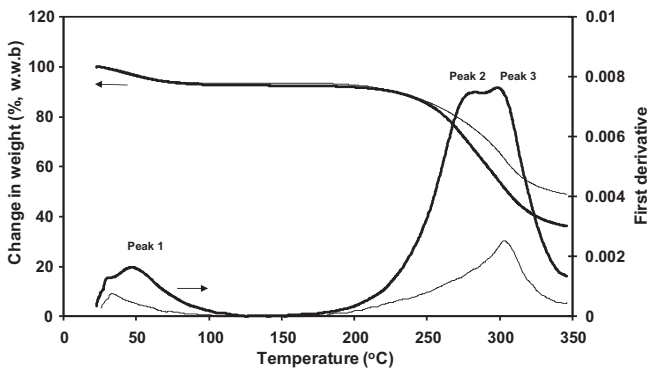

Fig. 2. Thermogravimetric analysis of AX powder (thick line) and lyophilised AX hydrogel (thin line).

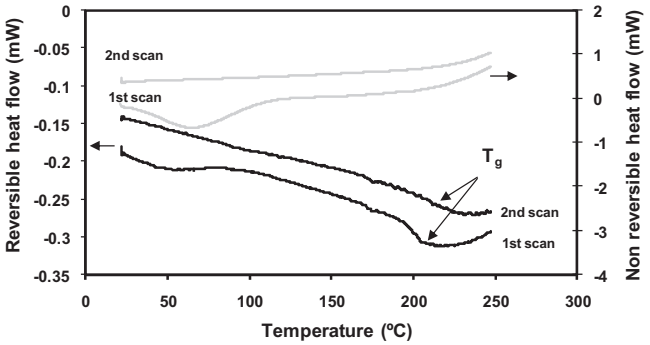

Fig. 3. MTDSC scans of AX powder showing the reversible and non-reversible heat flows.

MTDSC was carried out on AX powder but could not be achieved on the lyophilized AX hydrogels. Indeed filling the pan in order to establish a good contact between the sample and the bottom of the pan proved difficult. Therefore the following analysis only pertains to the AX powder tested as is. The reversible and non-reversible heat flow for AX powder tested as are shown in Fig. 3. During the first scan, there is a clear endothermic event at 70.9 ± 2.73 °C on the non-reversible heat flow indicating the removal of water confirmed by the TGA results. Further a sudden change in the base line of the reversible heat flow is observed at 198.8 ± 1.03 °C and is associated to the glass transition temperature, T_g. During the second scan this T_g is shifted towards high temperature values. For this particular type of pan, even sealed, water removal could not be entirely prevented as reported by Jang and Pyun (1996). As water would act as a plasticizer, its likely removal during the first scan would result in an increase in T_g values. Above 150 °C, the non-reversible heat flow is featureless. It is also interesting to note that above 250 °C, decomposition of the biopolymers is likely to occur. The confirmation of T_g is supported by the presence of a maximum in the first derivative of the reversible heat flow (data not shown). This is comparable with published values reported by Georget, Ng, Smith, and Waldron (1999) and Fessas and Schiraldi (2001). It is well known that T_g will depend on the molecular weight of the polymers, the side chains, the degree of cross-linking and the level of plasticizer. Nevertheless, it is noteworthy that the T_g found in the present study falls within an envelope of values taken from the literature for similar polysaccharides. After T_g the sample starts to degrade as demonstrated by the TGA results.

3.4. FT-IR

FT-IR spectra of AX powder, lyophilized AX hydrogel and caffeine are presented in Fig. 4. Scan for AX powder shows a typical absorbance region between 1200 and 900 cm^{-1} characteristic of polysaccharides consistent with the published results from Robert, Marquis, Barron, Guillon, and Saulnier (2005) and Kačuráková et al. (1999). The spectrum from caffeine has sharp peaks evidencing the crystalline structure of this molecule, similar to the results reported by Ucun, Sağlam, and Güçlü (2007). The lyophilized AX hydrogel has a similar spectrum to the AX powder with broad absorbance peak between 1200 and 900 cm^{-1} due the AX polymers and sharp peaks between 1700 and 1500 cm^{-1} are detected more likely originated from caffeine. A close examination of the FT-IR spectrum of the cross-linked materials reveals that AX polymers are not greatly affected by the cross-linking and the lyophilisation process. It is

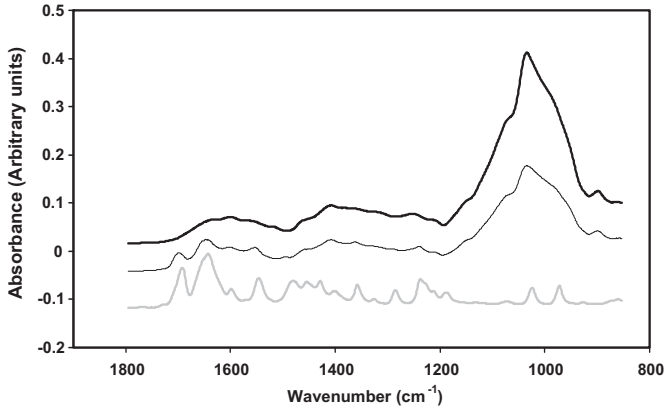

Fig. 4. FTIR spectra of caffeine (grey line), lyophilised AX hydrogel containing caffeine (thin black line) and AX powder (thick black line).

noteworthy that given the low level of caffeine (4.8% (w/w)) after lyophilisation, FT-IR is able to detect the drug in the lyophilised cross-linked material.

3.5. Swelling of AX hydrogels

Swelling of AX hydrogels containing caffeine fabricated with peroxidase concentration of 88 μg/g (AX basis) was carried out in distilled water and 0.1 M HCl to compare with the gastrointestinal fluid (Fig. 5). Over a period of 3 h, the greatest swelling was observed in water and reached a value of approximately 250% and 5% of the initial weight in distilled water and 0.1 M HCl, respectively. To investigate the mechanism of swelling in water, the data extracted from the change in weight as a function of time was fitted using the model from Ritger and Peppas (1987). When plotting the natural log values (data not shown) the diffusion exponent '*n*' was found to be 0.67 suggesting an anomalous diffusion mechanism indicating that water diffusion and polymer relaxation are occurring concomitantly. In contrast in 0.1 M HCl there was an initial increase in swelling to circa 5% and this remained unchanged during the treatment. The Ritger and Peppas equation could not model the swelling behaviour of the hydrogels in acidic conditions. However the data of the present study seem to be consistent with the work from İmren, Gümüşderelioğlu, and Güner (2009) who reported that cross-linked dextran hydrogels swelled the least at pH = 2 whereas at pH = 7 the swelling was the greatest. They interpreted their results by the protonation of the biopolymers at acidic pH leading to the formation of hydrogen bondings with proton accepting functional groups such as hydroxyls. And in the case

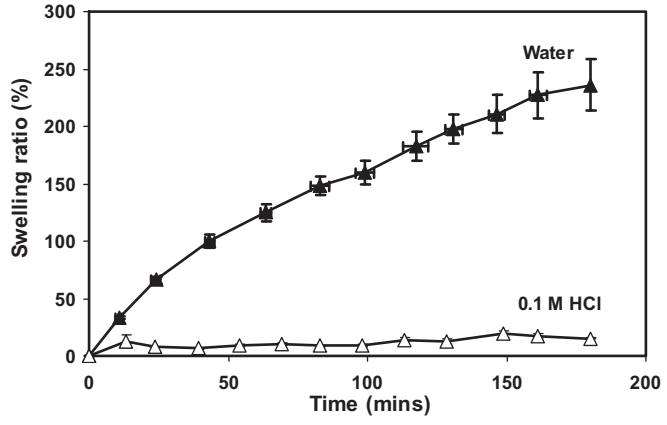

Fig. 5. Swelling of AX hydrogels in water and 0.1 M HCl. Error bars represent the standard error of the mean.

Table 1
Distance at failure, force at failure and area to failure for AX hydrogels variously oxidatively cross-linked. Within the same column, mean values sharing a letter in the superscript are not significantly different at the 0.05 level according to the Bonferroni test.

Enzyme (μg/g)	Distance at failure (mm)	Force at failure (N)	Area to failure (N mm)
88	$9.04 \pm 0.667^{a,d}$	$0.14 \pm 0.025^{a,b}$	$0.29 \pm 0.054^{a,b}$
176	9.89 ± 0.347^{a}	0.25 ± 0.057^{a}	0.35 ± 0.041^{a}
264	$8.96 \pm 0.425^{a,c}$	$0.14 \pm 0.022^{a,b}$	0.30 ± 0.042^{a}
352	6.41 ± 0.521^{b}	0.05 ± 0.010^{b}	0.09 ± 0.023^{b}
440	$7.00 \pm 0.758^{b,c,d}$	$0.12 \pm 0.055^{a,b}$	$0.19 \pm 0.078^{a,b}$

of AX hydrogels this might occur as once protonation takes place, hydroxyl functional groups from the xylose, arabinose or methoxy from ferulic acid might act as proton acceptors. Consequently this would hinder water ingress and swelling of the gels.

3.6. Mechanical properties of AX hydrogels

The mechanical properties of AX hydrogels prepared with 88–440 μg/g (AX basis) of horseradish peroxidase were determined and results are shown in Table 1. When peroxidase concentration increased from 88 μg/g to 264 μg/g, the distance to failure was approximately constant and decreased when enzyme concentration further increased. This is also accompanied by a similar behaviour for the force at failure. The values for the force at failure were converted into a more meaningful engineering value that is strength, by dividing the force values by the surface area of the probe. The values lie between 7.12 kN m^{-2} and 35.60 kN m^{-2}. The strength of AX hydrogels is comparable to that for galactomannan (Doyle, Giannouli, Martin, Brooks, & Morris, 2006; Sandolo et al., 2007) and xyloglucan gels (Miyazaki et al., 1998) but less than that for high methoxylated pectin gels (Genovese, Ye, & Singh, 2010). The degree of cross-linking, the molecular weight, the chemical structure and the presence of ionized functional groups will have a significant effect on the strength. The probe diameter will also influence the value for strength as reported by Ross and Scanlon (1999). With increasing indenter diameter the strength increases. It demonstrates that the mechanical properties of AX hydrogels can be modified though not significantly affected and this can be of use for biomedical applications. The area under the curve until the gel fails has also been calculated (Table 1). Again with a peroxidase concentration below 264 μg/g, the area under the curve to failure was approximately constant. For concentration greater than that, it decreases. The area under the curve is an indirect measure of the gel cohesiveness. This concentration value of 264 μg/g is critical. A similar phenomenon was reported by Kuuva, Lantto, Reinikainen, Buchert, & Autio (2003) who investigated the effect of laccase on sugar beet pectin gels. When testing the gels in compression, they found that the hardness increased up to laccase 100 nkat/g and then decreased. No possible explanation for this effect was put forward. However since the horseradish peroxidase/hydrogen peroxide ratio was kept constant, as the level of peroxide increased so did the ratio between hydrogen peroxide and ferulic monomer. This excess of hydrogen peroxide relative to ferulic might lead to an excess of radicals which might react with horseradish peroxidase (Huang et al., 2005). Hence it can be postulated that the oxidative cross-linking will be hindered and this is reflected by a decrease in deformation to failure, maximum force to failure and cohesiveness.

3.7. Caffeine dissolution

Fig. 6 shows the dissolution profiles of caffeine for AX hydrogels using horseradish peroxidase 88 μg/g (AX basis) in distilled water and 0.1 M HCl. The results show that, in the first 25 min,

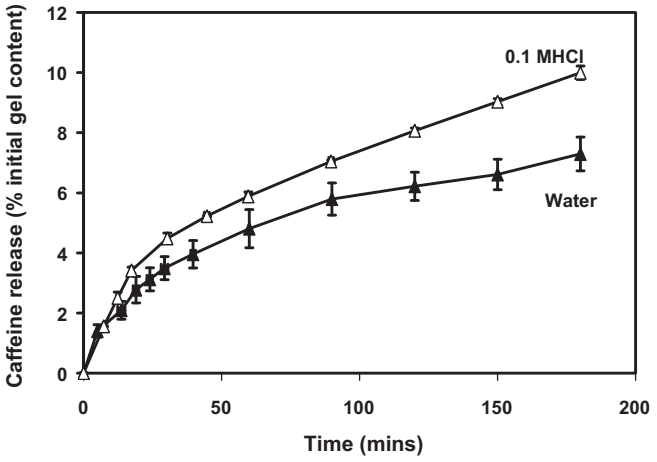

Fig. 6. Caffeine release from AX hydrogels in water and in 0.1 M HCl. Error bars represent the standard error of the mean.

approximately between 4% and 5% of the caffeine is rapidly released followed by a steady release to 7% and 10% of caffeine in distilled water and 0.1 M HCl, respectively. The caffeine dissolution profile from the AX hydrogels after 3 h was almost linear and still low. This would imply that in the case of caffeine, a minimum of active ingredient would be release in the stomach though not entirely with the reminder of the drug possibly dissolved later. The residence time in the stomachal fluid is approximately 30 min in an unfed state. Therefore AX hydrogels would show some potential for drug delivery in the low part of the gastro-intestinal tract.

In order to better understand the caffeine release mechanism, data from the dissolution profiles were fitted mathematically by applying the Higuchi equation which is as follows:

$$\frac{M_\infty}{M_o} = kt^{0.5}$$

where M_∞/M_o is the cumulative drug release ratio, k a kinetic constant and t the time for drug release. A second more generalized model has been applied to fit the dissolution experimental data and is based on the Ritger and Peppas equation (Ritger & Peppas, 1987) which is as follows:

$$\frac{M_\infty}{M_o} = kt^n$$

where M_∞/M_o was defined earlier, n is the release exponent indicative of the mechanism of drug release and k is the kinetic constant. A third equation proposed by Peppas and Sahlin (1989) has also been fitted to the experimental results and is as follows:

$$\frac{M_\infty}{M_o} = k_1 t^m + k_2 t^{2m}$$

where M_∞/M_o was defined earlier, k_1 and k_2 are the kinetic constants associated with diffusional and relaxational release, respectively and m is the purely Fickian diffusion exponent.

Table 2 shows the results of the fitting. For the Higuchi model, the k value is the greatest when AX hydrogels are treated in 0.1 M HCl. When applying the Ritger and Peppas model, n values lie around 0.5 implying that the mechanism of drug release is governed by Fickian diffusion. The more empirical model, that of Peppas and Sahlin when applied, shows that when forcing the diffusion coefficient m to equal 0.45, k_1 due to diffusional release is the greatest when compared to k_2 values and was the greatest in 0.1 M HCl. A similar phenomenon is detected when values of m are not constrained. Based on these results, caffeine dissolution in distilled water follows a Fickian diffusion mechanism with no polymer relaxation. As previously observed in distilled water AX hydrogels swelled significantly and this was accompanied by the caffeine release. In acidic condition (0.1 M HCl) caffeine release was the greatest and can also be explained by Fickian diffusion. There is a small contribution from the polymer erosion (see k_2 value in the Peppas and Sahlin model with $m = 0.45$). However the swelling is not as significant as described earlier but erosion of the AX polysaccharides is the more likely cause to explain the greatest release of caffeine. The erosion can be governed by AX hydrolysis as suggested by the work from Van Craeyveld, Delcour, and Courtin (2009). They found that at low pH, arabinoxylan polysaccharides undergo hydrolysis with the preferential release of arabinofuranosyl groups. In the present case, in 0.1 M HCl, AX hydrogel would degrade favoring more caffeine release when compared to the dissolution in distilled water.

4. Conclusions

AX powder properties were studied and the results revealed that AX biopolymers in a dry state have a T_g comparable to that of similar polysaccharides. It is fairly stable and only undergoes thermal decomposition at temperature above 250 °C. This has some bearing on the storage and processing of the material. Thermal stability is very important as AX polysaccharides can be used without compromising their functionality. With a view to develop AX based biomedical devices, powder could be subjected to sterilization by heating without causing irreversible effects. The oxidatively cross-linked AX hydrogels showed that for enzyme concentration greater than 264 μg/g (AX basis), the mechanical properties of the gels were to some degree impinged. This would suggest that the method of preparation is crucial and should be carefully controlled. In distilled water, AX hydrogels significantly swelled but caffeine release was the lowest whereas the swelling was the least and the caffeine dissolution was the greatest in 0.1 M HCl. The underlying mechanism during swelling is mainly governed by diffusion and polymer relaxation in distilled water but in acidic condition protonation of the AX polymers might hinder water ingress. The drug dissolution relies on diffusion in distilled water whereas in 0.1 M HCl erosion due to AX hydrolysis results in the greatest caffeine release. This work is the first study on the physical properties of AX powder and also demonstrates that oxidatively cross-linked AX hydrogels containing low molecular weight active component show some potential as controlled drug release device. Based on our findings, AX hydrogels seem to be an ideal candidate to encapsulate acid labile therapeutic molecules which necessitate reaching the lower part of the gastro-intestinal tract. This could expand the palette of applications for AX polysaccharides not only for protein delivery but also for simpler molecules.

Table 2
Release exponent (n), kinetic constant (k), diffusional (k_1) and relaxational (k_2) kinetic constants and purely Fickian diffusional exponent (m) for the dissolution of caffeine in water and 0.1 M HCl.

Medium	Higuchi		Ritger and Peppas			Peppas and Sahlin ($m = 0.45$)			Peppas and Sahlin			
	k	R^2	n	k (min^{-n})	R^2	k_1	k_2	R^2	k_1	k_2	m	R^2
H_2O	0.57 ± 0.050	0.968	0.47 ± 0.045	0.78 ± 0.193	0.990	0.75 ± 0.132	0.00 ± 0.011	0.990	0.53 ± 0.151	−0.01 ± 0.006	0.60 ± 0.051	0.995
0.1 M HCl	0.74 ± 0.003	0.991	0.50 ± 0.021	0.76 ± 0.072	0.992	0.83 ± 0.056	0.01 ± 0.007	0.992	0.63 ± 0.037	0.00 ± 0.003	0.57 ± 0.021	0.994

References

Berlanga-Reyes, C. M., Carvajal-Millán, E., Lizardi-Mendoza, J., Rascón-Chu, A., Marquez-Escalante, J. A., & Martínez-López, A. L. (2009). Maize arabinoxylan gels as protein delivery matrices. *Molecules*, *14*, 1475–1482.

British Pharmacopoeia (2010). *Medicines and Healthcare Products Regulatory Agency*, London, UK.

Bunzel, M., Ralph, J., Funk, C., & Steinhart, H. (2005). Structural elucidation of new ferulic acid-containing phenolic dimers and trimers isolated from maize bran. *Tetrahedron Letters*, *46*, 5845–5850.

Cao, N., Fu, Y., & He, J. (2007). Mechanical properties of gelatin films cross-linked, respectively, by ferulic acid and tannin acid. *Food Hydrocolloids*, *21*, 575–584.

Carvajal-Millan, E., Guilbert, S., Doublier, J.-L., & Micard, V. (2006). Arabinoxylan/protein gels: Structural, rheological and controlled release properties. *Food Hydrocolloids*, *20*, 53–61.

Carvajal-Millan, E., Guilbert, S., Morel, M.-H., & Micard, V. (2005). Impact of the structure of arabinoxylan gels on their rheological and protein transport properties. *Carbohydrate Polymers*, *60*, 431–438.

Carvajal-Millan, E., Landillon, V., Morel, M.-H., Rouau, X., Doublier, J.-L., & Micard, V. (2005). Arabinoxylan gels: Impact of the feruloylation degree on their structure and properties. *Biomacromolecules*, *6*, 309–317.

Courtin, C. M., & Delcour, J. A. (2001). Relative activity of endoxylanases towards water-extractable and water-unextractable arabinoxylan. *Journal of Cereal Science*, *33*, 301–312.

Cozic, C., Picton, L., Garda, M.-R., Marlhoux, F., & Le Cerf, D. (2009). Analysis of arabic gum: Study of degradation and water desorption processes. *Food Hydrocolloids*, *23*, 1930–1934.

Doyle, J. P., Giannouli, P., Martin, E. J., Brooks, M., & Morris, E. R. (2006). Effect of sugars, galactose content and chainlength on freeze-thaw gelation of galactomannans. *Carbohydrate Polymers*, *64*, 391–401.

Ebringerová, A., & Heinze, T. (2000). Xylan and xylan derivatives – biopolymers with valuable properties. 1. Naturally occurring xylans structures, isolation procedures and properties. *Macromolecular Rapid Communications*, *21*, 542–556.

Fessas, D., & Schiraldi, A. (2001). State diagrams of arabinoxylan–water binaries. *Thermochimica Acta*, *370*, 83–89.

Genovese, D. B., Ye, A., & Singh, H. (2010). High methoxyl pectin/apple particles composite gels: Effect of particle size and particle concentration on mechanical properties and gel structure. *Journal of Texture Studies*, *41*, 171–189.

Georget, D. M. R., Ng, A., Smith, A. C., & Waldron, K. W. (1999). Thermal characterisation of oxidatively cross-linked American corn bran hemicellulose. *Journal of the Science of Food and Agriculture*, *79*, 481–483.

Grabber, J. H., Ralph, J., & Hatfield, R. D. (2000). Cross-linking of maize walls by ferulate dimerization and incorporation into lignin. *Journal of Agricultural and Food Chemistry*, *48*, 6106–6113.

Höije, A., Sternemalm, E., Heikkinen, S., Tenkanen, M., & Gatenholm, P. (2008). Material properties of films from enzymatically tailored arabinoxylans. *Biomacromolecules*, *9*, 2042–2047.

Huang, Q., Huang, Q., Pinto, R. A., Griebenow, K., Schweitzer-Stenner, R., & Weber, W. J., Jr. (2005). Inactivation of horseradish peroxidase by phenoxyl radical attack. *Journal of the American Chemical Society*, *127*, 1431–1437.

İmren, D., Gümüşderelioğlu, M., & Güner, A. (2009). *In vitro* release kinetics of bovine serum albumin from highly swellable dextran hydrogels. *Journal of Applied Polymer Science*, *115*, 740–747.

Jang, J. K., & Pyun, Y. R. (1996). Effect of moisture content on the melting of wheat starch. *Starch*, *48*, 48–51.

Kačuráková, M., Wellner, N., Ebringerová, A., Hromádková, Z., Wilson, R. H., & Belton, P. S. (1999). Characterisation of xylan-type polysaccharides and associated cell wall components by FT-IR and FT-Raman spectroscopies. *Food Hydrocolloids*, *13*, 35–41.

Kuuva, T., Lantto, R., Reinikainen, T., Buchert, J., & Autio, K. (2003). Rheological properties of laccase-induced sugar beet pectin gels. *Food Hydrocolloids*, *17*, 679–684.

Miraftab, M., Qiao, Q., Kennedy, J. F., Anand, S. C., & Groocock, M. R. (2003). Fibres for wound dressings based on mixed carbohydrate polymer fibres. *Carbohydrate Polymers*, *53*, 225–231.

Miyazaki, S., Suisha, F., Kawasaki, N., Shirakawa, M., Yamatoya, K., & Attwood, D. (1998). Thermally reversible xyloglucan gels as vehicles for rectal drug delivery. *Journal of Controlled Release*, *56*, 75–83.

Ng, A., Greenshields, R. N., & Waldron, K. W. (1997). Oxidative cross-linking of corn bran hemicellulose: Formation of ferulic acid dehydrodimers. *Carbohydrate Research*, *303*, 459–462.

Niño-Medina, G., Carvajal-Millán, E., Rascon-Chu, A., Marquez-Escalante, J. A., Guerrero, V., & Salas-Muñoz, E. (2010). Feruloylated arabinoxylans and arabinoxylan gels: Structure, sources and applications. *Photochemistry Reviews*, *9*, 111–120.

Ou, S., & Kwok, K.-C. (2004). Ferulic acid: Pharmaceutical functions, preparation and applications in foods. *Journal of the Science of Food and Agriculture*, *84*, 1261–1269.

Peppas, N. A., & Sahlin, J. J. (1989). A simple equation for the description of solute release. III. Coupling of diffusion and relaxation. *International Journal of Pharmaceutics*, *57*, 169–172.

Péroval, C., Debeaufort, F., Despré, D., & Voilley, A. (2002). Edible arabinoxylan-based films. 1. Effects of lipid type on water vapor permeability, film structure, and other physical characteristics. *Journal of Agricultural and Food Chemistry*, *50*, 3977–3983.

Ritger, P. L., & Peppas, N. A. (1987). A simple equation for description of solute release. II. Fickian and anomalous release from swellable devices. *Journal of Controlled Release*, *5*, 37–42.

Robert, P., Marquis, M., Barron, C., Guillon, F., & Saulnier, L. (2005). FT-IR investigation of cell wall polysaccharides from cereal grains. Arabinoxylan infrared assignment. *Journal of Agricultural and Food Chemistry*, *53*, 7014–7018.

Ross, K. A., & Scanlon, M. G. (1999). Analysis of the elastic modulus of agar gel by indentation. *Journal of Texture Studies*, *30*, 17–27.

Sandolo, C., Matricardi, P., Alhaique, F., & Coviello, T. (2007). Dynamo-mechanical and rheological characterization of guar gum hydrogels. *European Polymer Journal*, *43*, 3355–3367.

Saulnier, L., Sado, P.-E., Branlard, G., Charmet, G., & Guillon, F. (2007). Wheat arabinoxylans: Exploiting variation in amount and composition to develop enhanced varieties. *Journal of Cereal Science*, *46*, 261–281.

Saulnier, L., & Thibault, J.-F. (1999). Ferulic acid and diferulic acids as components of sugar-beet pectins and maize bran heteroxylans. *Journal of the Science of Food and Agriculture*, *79*, 396–402.

Shen, D. K., Gu, S., & Bridgwater, A. V. (2010). Study on the pyrolytic behaviour of xylan-based hemicellulose using TG-FTIR and Py-GC-FTIR. *Journal of Analytical and Applied Pyrolysis*, *87*, 199–206.

Simi, C. K., & Abraham, T. E. (2010). Biodegradable biocompatible xyloglucan films for various applications. *Colloid and Polymer Science*, *288*, 297–306.

Tuvikene, R., Truus, K., Kollist, A., Volobujeva, O., Mellikov, E., & Pehk, T. (2008). Gel-forming structures and stages of red algal galactans of different sulfation levels. *Journal of Applied Phycology*, *20*, 527–535.

Ucun, F., Sağlam, A., & Güçlü, V. (2007). Molecular structures and vibrational frequencies of xanthine and its methyl derivatives (caffeine and theobromine) by ab initio Hartree-Fock and density functional theory calculations. *Spectrochimica Acta Part A*, *67*, 342–349.

Van Craeyveld, V., Delcour, J. A., & Courtin, C. M. (2009). Extractability and chemical and enzymic degradation of psyllium (Plantago ovata Forsk) seed husk arabinoxylans. *Food Chemistry*, *112*, 812–819.

Vázquez, M. J., Pérez-Marcos, B., Gómez-Amoza, J. L., Martínez-Pacheco, R., Souto, C., & Concheiro, A. (1992). Influence of technological variables on release of drugs from hydrophilic matrices. *Drug Development and Industrial Pharmacy*, *18*, 1355–1375.

Vendruscolo, C. W., Ferrero, C., Pineda, E. A. G., Silveira, J. L. M., Freitas, R. A., Jiménez-Castellanos, M. R., & Bresolin, T. M. B. (2009). Physicochemical and mechanical characterization of galactomannan from *Mimosa scabrella*: Effect of drying method. *Carbohydrate Polymers*, *76*, 86–93.